

Study of Hopf bifurcation of delayed tritrophic system: dinoflagellates, mussels, and crabs

Hafdane M.¹, Agmour I.¹, El Foutayeni Y.^{1,2}

¹*Analysis, Modeling and Simulation Laboratory, Hassan II University, Morocco*

²*Unit for Mathematical and Computer Modeling of Complex Systems, IRD, France*

(Received 14 April 2022; Revised 24 September 2022; Accepted 31 October 2022)

In this paper, we have a discrete delayed dynamic system of three marine species: prey, predator, and superpredator. In addition to the effect of prey toxicity, we consider the negative fishing effect of these species. The study of this model consists of the search for equilibria with eigenvalue analysis, the existence of Hopf bifurcations at interior equilibria, and the determination of direction and stability analysis of Hopf bifurcation using the theory of normal form and center manifold. Some examples are given with numerical simulations to illustrate the results in different cases of delay.

Keywords: *predator–prey; stability analysis; Hopf bifurcation; discrete delay; fishing effort.*

2010 MSC: 91B05, 91A06, 91B02, 91B50

DOI: 10.23939/mmc2023.01.066

1. Introduction

The aquatic life remains one of the fundamental biological phenomena that make our planet habitable since it represents a vital resource manageable for a sustainable future. Morocco, a country bordered by the Atlantic Ocean in the west and the Mediterranean in the north, embodies both a rich marine biodiversity and a challenge for the preservation of these resources against human overfishing, but also from their degradation due to the presence of toxins such as those contained in dinoflagellates used in pharmacology and cosmetics.

Indeed, the mussels date back 250 million years with an ancient origin in the Moroccan coasts. The geology demonstrates their resilience to climatic changes, and they feed on these dinoflagellates, while crabs feed on both of them, forming a food chain of a tritrophic system.

On the one hand, mussels are able to filter out the toxicity of dinoflagellates. Still, this filtration causes a high concentration of toxins in the body of mussels. Therefore, toxicity can affect crabs either from mussels or from dinoflagellates directly. On the other hand, following the world health organization, humans, while consuming crabs and mussels, become affected by this toxicity which can compromise their nervous system.

For the reasons outlined, this paper proposes a study of a delayed bioeconomic model for three marine species. The proposed model illustrates the importance of delay in studying mathematical models as a case study. According to the literature, the theory of delay differential equations has developed extensively, especially with Belman and Cooke (1963); Hale (1977), which has made it possible to model some complicated phenomena in a more realistic manner. As part of the study of bioeconomic models for marine species, reference can be made to [1–8]. In these papers, the authors studied, constructed and analyzed several bioeconomic models while taking into account the fishing of the species in question. Their goal was to maximize harvester returns while ensuring the sustainability of marine resources. They also carried out numerical simulations of the variation of bioeconomic parameters and number of fishermen.

In the context of delayed biomathematic models one can cite [9–11]. The authors of this paper studied Hopf bifurcation for a prey–predator model. In the numerical simulation part, they discussed

only one case. The novelty of this paper remains in the proposal and the study of a delayed model for marine species of Moroccan coastal zone as an exploitable species with economic importance. Mathematically, this toxicity is represented by delay. Moreover, in this paper, we give interest to the study of Hopf bifurcation, since it represents the qualitative change in the state of the system.

The paper is structured as follows: following Introduction, the proposed bioeconomic model is presented in Section 1. In Section 2, we study the existence, the positivity and the limitations of the system's solutions. In Section 3, the stability of the interior equilibrium point is analysed according to the value of τ_1 and τ_2 , then the appearance of Hopf bifurcation is discussed. In Section 4, we study the stability and direction of Hopf bifurcation, the result of the preceding sections. In Section 5, numerical simulations of theoretical results obtained are presented.

2. Presentation of the model

The following system presents a food chain of three marine species living in the same environment, the growth of each species is modelled by Verhulst logistic equation and interactions between them by Lotka Volterra predation version. The variables d , m and c present the densities of toxic dinoflagellates, mussels and crabs, respectively. The quantities caught for each species are defined by the coefficients $q_1 E_1 d$, $q_2 E_2 m$ and $q_3 E_3 c$, where q_i is the catchability coefficient of fish species and E_i is the fishing effort to exploit the species i .

In the system (1), we have the parameter τ . It represents the delay associated with toxicity. Biologically, we can explain it by the time necessary for crabs to get affected by toxins when feeding on mussels or dinoflagellates,

$$\begin{cases} \dot{d}(t) = r_1 d(1 - d/K) - \alpha_{12} dm - \alpha_{13} dc - q_1 E_1 d, \\ \dot{m}(t) = r_2 m(1 - m/K) + \beta_{21} dm - \beta_{23} mc - q_2 E_2 m, \\ \dot{c}(t) = r_3 c(1 - c/K) + \lambda_{31} dc + \lambda_{32} mc - \delta_1 d(t - \tau_1)c - \delta_2 m(t - \tau_2)c - q_3 E_3 c. \end{cases} \quad (1)$$

The following table summarizes the different parameters and their explanations.

Table 1. The meaning of biological parameters.

Parameter	Meaning
$\alpha_{12}, \alpha_{13}, \beta_{23}$	Mortality rates due to predation effect
$\beta_{21}, \lambda_{31}, \lambda_{32}$	Reproductive rates of predators based on prey encountered
δ_1, δ_2	Mortality rates by toxicity effect
r_i	Intrinsic growth rates
K	Carrying capacities for the species

3. Existence, positivity and boundedness of solution

In this section, we aim to study the existence, positivity and boundedness of the solution to system (1).

3.1. Positivity of solutions

Theorem 1. *The set $\{(d, m, c) \in \mathbb{R}^3 : d, m, c \geq 0\}$ is positively invariant for system.*

Proof. Note that the plans $x = 0$, $y = 0$ and $z = 0$ are invariant, indeed

$$\left. \frac{d}{dt} d(t) \right|_{d=0} = 0, \quad \left. \frac{d}{dt} m(t) \right|_{m=0} = 0, \quad \left. \frac{d}{dt} c(t) \right|_{c=0} = 0.$$

So, if we start with strictly positive initial points, the solutions do not exceed these plans and remain positive for any $t > 0$. So the set $\{(d, m, c) \in \mathbb{R}^3 : d, m, c \geq 0\}$ is positively invariant. ■

3.2. Boundedness of solutions

Theorem 2. *The solutions of system (1) are bounded.*

Proof. (i) We consider the following inequality

$$\frac{d}{dt}d(t) = r_1d(1 - d/K) - \alpha_{12}dm - \alpha_{13}dc - q_1E_1d \leq r_1d(1 - d/K).$$

By integrating, we obtain $d(t) \leq K$.

(ii) For m , we have

$$\begin{aligned} \frac{d}{dt}m(t) &= r_2m(1 - m/K) + \beta_{21}dm - \beta_{23}mc - q_2E_2m \\ &\leq r_2m(1 - m/K) + \beta_{21}Km \\ &\leq (r_2 + \beta_{21}K)m \left(1 - \frac{r_2m}{K(r_2 + \beta_{21}K)}\right). \end{aligned}$$

So, m is bounded.

(iii) For c , we have

$$\begin{aligned} \frac{d}{dt}c(t) &= r_3c(1 - c/K) + \lambda_{31}dc + \lambda_{32}mc - \delta_1d(t - \tau_1)c - \delta_2m(t - \tau_2)c - q_3E_3c \\ &\leq r_3c(1 - c/K) + \lambda_{31}dc + \lambda_{32}mc. \end{aligned}$$

We follow the same process to prove that c is bounded. ■

3.3. Existence and uniqueness of solution

The system (1) is represented by the following form: $\dot{x} = f(x(t), x(t - \tau_1), x(t - \tau_2))$, with $f = (f_1, f_2, f_3)^T$ and

$$\begin{aligned} f_1 &= r_1d(1 - d/K) - \alpha_{12}dm - \alpha_{13}dc - q_1E_1d, \\ f_2 &= r_2m(1 - m/K) + \beta_{21}dm - \beta_{23}mc - q_2E_2m, \\ f_3 &= r_3c(1 - c/K) + \lambda_{31}dc + \lambda_{32}mc - \delta_1d(t - \tau_1)c - \delta_2m(t - \tau_2)c - q_3E_3c. \end{aligned}$$

Theorem 3. *The system (1) admits a unique solution.*

Proof. The function f is continuous and f_i satisfy the following condition $\frac{\partial f_i}{\partial x_j}$, $i, j = 1, 2, 3$ are continuous and bounded.

Since the partial derivatives are continuous and bounded, then f is a Lipschitz function.

The conditions of Cauchy–Lipschitz are satisfied. Therefore, according to the fundamental theorem of functional differential equations cited in [12], the existence and uniqueness of the system solution are confirmed. ■

4. Stability analysis

The main objective of this section is to determine the interior equilibria of system (1) and to discuss its stability according to the delay parameter.

4.1. Search for equilibrium points

Theorem 4. *The system (1) admits a unique strictly positive equilibrium point $P^*(d^*, m^*, c^*)$.*

Proof. When replacing $\dot{d}(t)$, $\dot{m}(t)$ and $\dot{c}(t)$ by 0 and after dividing the equations by d , m and c respectively, we obtain the following linear system

$$\begin{cases} \frac{r_1}{k}d^* + \alpha_{12}m^* + \alpha_{13}c^* = V_1, \\ \frac{r_2}{k}m^* - \beta_{21}d^* + \beta_{23}c^* = V_2, \\ \frac{r_3}{k}c^* + B_1d^* + B_2m^* = V_3 \end{cases} \quad (2)$$

with $V_i = r_i - q_i E_i$ and $B_i = \delta_i - \lambda_{3i}$.

By resolving the system (2), we obtain the interior equilibrium point $P^*(d^*, m^*, c^*)$. ■

4.2. Study of local stability

4.2.1. System without delay

Theorem 5. The interior equilibrium point (d^*, m^*, c^*) is locally asymptotically stable if $h_2 > 0$, $h_1 > 0$, $h_0 > 0$ and $h_1 h_2 - h_0 > 0$.

Proof. To linearize the system, the following variable substitutions are made: $D = d - d^*$, $M = m - m^*$ and $C = c - c^*$. We obtain the following system

$$\begin{cases} \dot{D} = \frac{-r_1}{K}d^*D - \alpha_{12}d^*M - \alpha_{13}d^*C - \frac{r_1}{K}D^2 - \alpha_{12}DM - \alpha_{13}DC, \\ \dot{M} = -\frac{r_2}{K}m^*M + \beta_{21}m^*D - \beta_{23}m^*C - \frac{r_2}{K}M^2 + \beta_{21}MD - \beta_{23}MC, \\ \dot{C} = (\lambda_{31}D + \lambda_{32}M - \frac{r_3}{K}C)c^* + (\lambda_{31}D + \lambda_{32}M - \frac{r_3}{K}C)C \\ \quad - [\delta_1 D(t - \tau_1) + \delta_2 M(t - \tau_2)]c^* - [\delta_1 D(t - \tau_1) + \delta_2 M(t - \tau_2)]C. \end{cases} \quad (3)$$

We consider the following equation

$$\det(XI - A_0 - A_1 e^{-X\tau_1} - A_2 e^{-X\tau_2}) = 0 \quad (4)$$

with

$$A_0 = \begin{pmatrix} -\frac{r_1}{K}d^* & -\alpha_{12}d^* & -\alpha_{13}d^* \\ \beta_{21}m^* & -\frac{r_2}{K}m^* & -\beta_{23}m^* \\ \lambda_{31}c^* & \lambda_{32}c^* & -\frac{r_3}{K}c^* \end{pmatrix}, \quad A_1 = \begin{pmatrix} 0 & 0 & 0 \\ 0 & 0 & 0 \\ -\delta_1 c^* & 0 & 0 \end{pmatrix}, \quad A_2 = \begin{pmatrix} 0 & 0 & 0 \\ 0 & 0 & 0 \\ 0 & -\delta_2 c^* & 0 \end{pmatrix}.$$

By solving the equation (4), we obtain the following equality

$$X^3 + a_1 X^2 + a_2 X + a_3 + (b_1 X + b_2) e^{-X\tau_1} + (c_1 X + c_2) e^{-X\tau_2} = 0. \quad (5)$$

The coefficients are represented in Table 2.

Table 2. Expressions for the coefficients in (5).

Coefficient	Expression
a_1	$\frac{r_2}{K}m^* + \frac{r_3}{K}c^* + \frac{r_1}{K}d^*$
a_2	$\frac{r_2 r_3}{K^2}m^*c^* + \beta_{23}\lambda_{32}m^*c^* + \frac{r_1 r_2}{K^2}d^*m^* + \frac{r_1 r_3}{K^2}d^*c^* + \beta_{21}\alpha_{12}d^*m^* + \alpha_{13}\lambda_{31}d^*c^*$
a_3	$\frac{r_1 r_2 r_3}{K^3}d^*m^*c^* + \frac{r_1}{K}\beta_{23}\lambda_{32}d^*m^*c^* + \alpha_{12}\beta_{21}\frac{r_3}{K}d^*m^*c^* + \beta_{21}\alpha_{13}\lambda_{32}d^*m^*c^* - \alpha_{12}\beta_{23}\lambda_{31}d^*m^*c^* + \alpha_{13}\lambda_{31}\frac{r_2}{K}d^*m^*c^*$
b_1	$-\alpha_{13}\delta_1 d^*c^*$
b_2	$\delta_1 \alpha_{12} \beta_{23} d^* m^* c^* - \delta_1 \alpha_{13} \frac{r_2}{K} d^* m^* c^*$
c_1	$-\beta_{23} \delta_2 m^* c^*$
c_2	$-\alpha_{13} \delta_2 \beta_{21} d^* m^* c^* - \frac{r_1}{K} \beta_{23} \delta_2 d^* m^* c^*$

By replacing $\tau_1 = 0$ and $\tau_2 = 0$, the equation (5) becomes

$$X^3 + h_2X^2 + h_1X + h_0 = 0$$

with $h_2 = a_1$, $h_1 = a_2 + b_1 + c_1$ and $h_0 = a_3 + b_2 + c_2$.

We have $h_2 > 0$, $h_1 > 0$, $h_0 > 0$ and if $h_1h_2 - h_0 > 0$, the Routh–Hurwitz conditions are verified. ■

4.2.2. System with a single delay

In the case: $\tau_1 > 0$ and $\tau_2 = 0$.

Theorem 6. (i) The positive equilibrium $P^*(d^*, m^*, c^*)$ is asymptotically stable for all $\tau_1 \geq 0$, if $r_1 \geq 0$ and $\Delta = s_3^2 - 3s_2 \leq 0$.

(ii) The positive equilibrium $P^*(d^*, m^*, c^*)$ is asymptotically stable for all $\tau_1 \in I$, if $s_1 \geq 0$, $\Delta = s_3^2 - 3s_2 > 0$, $v_1^* = (-s_3 + \sqrt{\Delta})/3 > 0$ and $g(v_1^*) \leq 0$, or $s_1 < 0$ and $g'(v_k) \neq 0$.

(iii) The system (2) undergoes a Hopf bifurcation at the equilibrium $P^*(d^*, m^*, c^*)$ when $\tau_1 = \tau_{1k}^{(j)}$ ($j = 0, 1, 2, \dots$) if all conditions stated in (ii) hold.

Proof. We replace τ_2 with 0 in our equation and we obtain

$$X^3 + a_1X^2 + (a_2 + c_1)X + a_3 + c_2 + (b_1X + b_2)e^{-X\tau_1} = 0. \quad (6)$$

It is assumed that the equation admits a complex solution $X = iw$ ($w > 0$)

$$\begin{cases} w^3 - (a_2 + c_1)w = -b_2 \sin w\tau_1 + b_1w \cos w\tau_1, \\ a_1w^2 - (a_3 + c_2) = b_2 \cos w\tau_1 + b_1w \sin w\tau_1. \end{cases}$$

The two equalities are squared to obtain the following system

$$\begin{cases} (w^3 - (a_2 + c_1)w)^2 = (b_1w \cos w\tau_1 - b_2 \sin w\tau_1)^2, \\ (a_1w^2 - (a_3 + c_2))^2 = (b_2 \cos w\tau_1 + b_1w \sin w\tau_1)^2. \end{cases}$$

By simple calculation we have

$$\begin{cases} w^6 - 2(a_2 + c_1)w^4 + (a_2 + c_1)w^2 = b_1^2w^2(\cos w\tau_1)^2 + b_2^2(\sin w\tau_1)^2 - 2b_1b_2w \cos w\tau_1 \cos w\tau_2, \\ a_1^2w^4 + (a_3 + c_2)^2 - 2(a_3 + c_2)a_1w^2 = b_1^2w^2(\sin w\tau_1)^2 + b_2^2(\cos w\tau_1)^2 + 2b_1b_2w \cos w\tau_1 \cos w\tau_2. \end{cases}$$

The sum of the first equation with the second one leads to the following equation

$$w^6 - 2(a_2 + c_1)w^4 + (a_2 + c_1)w^2 + a_1^2w^4 + (a_3 + c_2)^2 - 2(a_3 + c_2)a_1w^2 = b_1^2w^2 + b_2^2.$$

We simplify

$$w^6 + s_3w^4 + s_2w^2 + s_1 = 0. \quad (7)$$

The coefficients are represented in Table 3.

Table 3. Expressions for the parameters in (7).

Parameter	Expression
s_3	$a_1^2 - 2(a_2 + c_1)$
s_2	$(a_2 + c_1)^2 - 2a_1(a_3 + c_2) - b_1^2$
s_1	$(a_3 + c_2)^2 - b_2^2$

In order to simplify the calculations, we put $v = w^2$,

$$v^3 + s_3v^2 + s_2v + s_1 = 0. \quad (8)$$

Let

$$g(v) = v^3 + s_3v^2 + s_2v + s_1.$$

We have $g(0) = s_1$, $\lim_{v \rightarrow \infty} g(v) = +\infty$ and

$$g'(v) = 3v^2 + 2s_3v + s_2.$$

To discuss about the roots of the equation (8), we use the following lemma [11].

Lemma 1. For the polynomial Eq. (8), we have the following results

- Equation (8) has at least one positive root if $s_1 < 0$.
- Equation (8) has no positive roots if $s_1 \geq 0$, and $\Delta = s_3^2 - 3s_2 \leq 0$.
- Equation (8) has positive roots if $s_1 \geq 0$, $\Delta = s_3^2 - 3s_2 > 0$, $v_1^* = (-s_3 + \sqrt{\Delta})/3 > 0$ and $g(v_1^*) \leq 0$.

Without loss of generality, we suppose that Eq. (8) has three positive roots, denoted as v_1, v_2 and v_3 , respectively. Therefore, Eq. (7) has three positive roots $w_k = \sqrt{v_k}$, $k = 1, 2, 3$. The corresponding critical value of time delay $\tau_{1k}^{(j)}$:

$$\tau_{1k}^{(j)} = \frac{1}{w_k} \arccos \frac{b_1 w_k^4 + (a_1 b_2 - (a_2 + c_1) b_1) w_k^2 - (a_3 + c_2) b_2}{b_1^2 w_k^2 + b_2^2} + \frac{2j\pi}{w_k}.$$

Then $\pm i w_k$ is a pair of purely imaginary roots of Eq. (6) with $\tau_1 = \tau_{1k}^{(j)}$, $\tau_2 = 0$. Following Hopf bifurcation theorem [13], we must verify the transversality condition. Differentiating Eq. (6) with respect to τ_1 , and noticing that X is a function of τ_1 , it follows that

$$\left(\frac{dX}{d\tau_1} \right)^{-1} = \frac{(3X^2 + a_1 X + a_2 + c_1) e^{X\tau_1}}{X(b_1 X + b_2)} + \frac{b_1}{X(b_1 X + b_2)} - \frac{\tau_1}{\lambda}. \quad (9)$$

Thus

$$\operatorname{Re} \left(\frac{dX}{d\tau_1} \right)^{-1} = \operatorname{Re} \frac{(3X^2 + a_1 X + a_2 + c_1) e^{X\tau_1} + b_1}{X(b_1 X + b_2)}.$$

Notice that $\operatorname{sign} \left\{ \frac{d \operatorname{Re} X}{d\tau_1} \right\}_{X=iw_k} = \operatorname{sign} \left\{ \operatorname{Re} \left(\frac{dX}{d\tau_1} \right)^{-1} \right\}_{X=iw_k}$. Then

$$\begin{aligned} \operatorname{sign} \left\{ \frac{d \operatorname{Re} X}{d\tau_1} \right\}_{X=iw_k} &= \operatorname{sign} \left\{ \operatorname{Re} \left(\frac{dX}{d\tau_1} \right)^{-1} \right\}_{X=iw_k} \\ &= \operatorname{sign} \left\{ (3w_k^6 + 2r_3 w_k^4 + r_2 w_k^2) / (b_1^2 w_k^4 + b_2^2 w_k^2) \right\} \\ &= \operatorname{sign} \left\{ g'(v_k) v_k / (b_1^2 v_k^2 + b_2^2 v_k) \right\}. \end{aligned}$$

Therefore, $\left\{ \frac{d \operatorname{Re} X}{d\tau_1} \right\} \neq 0$ if $g'(v_k) \neq 0$. ■

Remark 1. If we have $\tau_1 = 0$ and $\tau_2 > 0$, or $\tau_1 = \tau_2 = \tau \neq 0$, we follow the same reasoning and we obtain the same results in the case of $\tau_1 > 0$ and $\tau_2 = 0$.

4.2.3. System with two delays

In the case: $\tau_2 > 0$, $\tau_1 \in I$ and $\tau_1 \neq \tau_2$

Theorem 7. (i) The positive equilibrium $P^*(d^*, m^*, c^*)$ is asymptotically stable for all $\tau_1 \in I$.

(ii) If Eq. (10) has at least finite positive root and $\left\{ \operatorname{Re} \left(\frac{d\lambda}{d\tau_1} \right)^{-1} \right\}_{\lambda=iw_i} \neq 0$, then system (2) undergoes a Hopf bifurcation at the equilibrium $P^*(d^*, m^*, c^*)$, when $\tau_2 = \tau_2^0$.

Proof. We suppose that $i\omega$ ($\omega > 0$) is the root of Eq. (5), then we obtain

$$\begin{cases} -\omega^3 + a_2\omega + b_1\omega \cos \omega\tau_1 - b_2 \sin \omega\tau_1 = c_2 \sin \omega\tau_2 - c_1\omega \cos \omega\tau_2, \\ a_1\omega^2 - a_3 - b_2 \cos \omega\tau_1 - b_1\omega \sin \omega\tau_1 = c_1\omega \sin \omega\tau_2 + c_2 \cos \omega\tau_2. \end{cases}$$

After explicit calculations, we have

$$\begin{aligned} \omega^6 + l_1\omega^4 + l_2\omega^2 + l_3 + [m_1\omega^3 + m_2\omega] \sin \omega\tau_1 \\ + [n_1\omega^4 + n_2\omega^2 + n_3] \cos \omega\tau_1 = 0. \end{aligned} \quad (10)$$

We suppose that Eq. (10) has at least one positive finite root. Without loss of generality, it is assumed that Eq. (10) has N positive roots, noted by ω_i , ($i = 1, 2, \dots, N$). Note that with Eq. (10) we obtain $\tau_{2i}^{(j)}$. Let $\tau_2^0 = \tau_{2i0}^{(0)} = \min\{\tau_{2i}^{(0)}\}$, $\omega_0 = \omega_{i0}$, and $\lambda(\tau_2) = \alpha(\tau_2) + i\omega(\tau_2)$ be the roots of Eq. (3) satisfying $\alpha(\tau_{2i}^{(j)}) = 0$, $\omega(\tau_{2i}^{(j)}) = \omega_i$.

Table 4. Expressions for the parameters in (10).

Parameter	Expression
l_1	$a_1^2 - 2a_2$
l_2	$a_2^2 - 2a_3a_1 + b_1^2 - c_1^2$
l_3	$a_3^2 + c_2^2 - c_2^2$
m_1	$2b_2 - 2b_1a_1$
m_2	$2b_1a_3 - 2b_2a_2$
n_1	$-2b_1$
n_2	$2b_1a_2 - 2b_2a_1$
n_3	$2a_3b_2$

Table 5. Expressions for the parameters in (11).

Parameter	Expression
Q_1	$c_2 b_1 + c_2 b_2 \tau_1 + c_1 b_1 \tau_1 w^2$
Q_2	$2a_1 c_2 - c_1 (-3w^2 + a_2)$
Q_3	$b_1 \tau_1 c_2 - c_1 b_2 \tau_1 - b_1 c_1$
Q_4	$2a_1 c_1 w^3 - c_2 w (-3w^3 + a_2)$

By calculating, we have

$$\left\{ \operatorname{Re} \left(\frac{d\lambda}{d\tau_2} \right)^{-1} \right\}_{\lambda=i\omega_i} = \frac{\Delta}{c_1^2 \omega_0^4 + c_2^2 \omega_0^2},$$

where

$$\Delta = Q_1 w \sin \omega_0 (\tau_1^* + \tau_2^0) + Q_2 w^2 \cos \omega_0 \tau_2^0 + Q_3 w^2 \cos \omega_0 (\tau_1^* + \tau_2^0) + Q_4 \sin \omega_0 \tau_2^0 - c_1 \omega_0^2. \quad (11)$$

If $\tau_1 > 0$, $\tau_2 \in I$ and $\tau_1 \neq \tau_2$, we have the same result. ■

5. Stability and direction of Hopf bifurcation

In the previous section, we found that our system is going through a Hopf bifurcation when $\tau_2 = \tau_2^0$, the purpose of this section is to study the direction of this bifurcation and the stability of the periodic solutions of our system using the theory of normal form and the center manifold theorem [13].

Theorem 8. For system (3), under loss of generalities, we assume that $\tau_2^0 > \tau_1^*$ and we have the following results:

- The direction of Hopf bifurcation is determined by the sign of η_2 ; if $\eta_2 > 0$ ($\eta_2 < 0$), then the Hopf bifurcation is supercritical (subcritical) and the periodic solutions exist for $\tau_2 > \tau_2^0$ ($\tau_2 < \tau_2^0$).
- The stability of the periodic solution is determined by the sign of β_2 : the bifurcations periodic solutions are orbitally asymptotically stable (unstable) if $\tau_2 > \tau_2^0$ ($\tau_2 < \tau_2^0$). The period of the periodic solutions is determined by the sign of T_2 : if $T_2 > 0$ ($T_2 < 0$), the periodic solutions increase (decrease).

Proof. Under loss of generalities, we assume that $\tau_2^0 > \tau_1^*$.

We put $\tau_2 = \tau_2^0 + \eta$, $\varphi_t(\theta) = \varphi(t + \theta) \in C$, $L_\eta: C \rightarrow \mathbb{R}^3$ and $F: \mathbb{R} \times C \rightarrow \mathbb{R}^3$.

We can express the system (3) as the following functional differential system in $C([- \tau_1^*, 0], \mathbb{R}^3)$

$$\dot{\varphi}(t) = L_\eta(\varphi_t) + f(\eta, \varphi_t), \quad (12)$$

where

$$L_\eta \chi = A_0 \chi(0) + A_1 \chi(-\tau_1^*) + A_2 \chi(-\tau_2^0)$$

and

$$f(\eta, \chi) = \begin{pmatrix} -\frac{r_1}{K} \chi_1^2(0) - \alpha_{12} \chi_1(0) \chi_2(0) - \alpha_{13} \chi_1(0) \chi_3(0) \\ -\frac{r_2}{K} \chi_2^2(0) + \beta_{21} \chi_1(0) \chi_2(0) - \beta_{23} \chi_2(0) \chi_3(0) \\ [-\frac{r_3}{K} \chi_3(0) + \lambda_{31} \chi_1(0) + \lambda_{32} \chi_2(0) - \delta_1 \chi_1(-\tau_1^*) - \delta_2 \chi_2(-\tau_2^0)] \chi_3(0) \end{pmatrix}.$$

By the representation of Riesz, we have the existence of a matrix of order 3 $g(\theta, \eta)$ of bounded variation for $\theta \in [-\tau_1^*, 0]$, which verifies

$$L_\eta \chi = \int_{-\tau_1^*}^0 dg(\theta, \eta) \chi(\theta), \quad \forall \chi \in C.$$

This matrix is written in the following form

$$g(\theta, \eta) = A_0 \delta(\theta) + A_1 \delta(\theta + \tau_1) + A_2 \delta(\theta + \tau_2^0),$$

where

$$\delta(\theta) = \begin{cases} 0, & \theta \neq 0, \\ 1, & \theta = 0. \end{cases}$$

For $\chi \in C^1([-\tau_1^*, 0], \mathbb{R}^3)$, we have

$$M(\eta)\chi = \begin{cases} \frac{d\chi(\theta)}{d\theta}, & \theta \in [-\tau_1^*, 0), \\ \int_{-\tau_1^*}^0 dg(\xi, \eta) \chi(\xi), & \theta = 0, \end{cases} \quad R(\eta)\chi = \begin{cases} 0, & \theta \in [-\tau_1^*, 0), \\ f(\eta, \chi), & \theta = 0. \end{cases}$$

So, we can write the system in the following form

$$\dot{\varphi}_t = M(\eta)\varphi_t + R(\eta)\varphi_t.$$

For $\chi \in C^1([0, 1], (\mathbb{R}^3)^*)$, the adjoint operator M^* of $M(0)$ is written as follows

$$M^*\chi = \begin{cases} -\frac{d\chi(s)}{ds}, & s \in (0, \tau_1^*], \\ \int_{-\tau_1^*}^0 dg^T(t, \theta) \chi(-t), & s = 0. \end{cases}$$

For $\chi \in C^1([-\tau_1^*, 0], \mathbb{R}^3)$ and $\psi \in C^1([0, 1], (\mathbb{R}^3)^*)$, we use the bilinear form

$$\langle \psi, \chi \rangle = \bar{\psi}^T(0)\chi(0) - \int_{-\tau_1^*}^0 \int_{\xi=0}^0 \bar{\psi}^T(\xi - \theta) dg(\theta) \chi(\xi) d\xi.$$

According to Section 3, $M(0)$ admits $\pm i\omega_0$ as eigenvalues, so they are also eigenvalues of M^* . In order to search for the expression of $M(0)$, it is assumed that $\rho(\theta) = \rho(0)e^{i\omega_0\theta}$ is its eigenvector associated with the eigenvalue $i\omega_0$. Therefore $M(0)$ is written as $M(0) = i\omega_0\rho(\theta)$.

When $\theta = 0$, we have the following equation

$$\left[i\omega_0 I - \int_{-\tau_1^*}^0 dg(\theta) e^{i\omega_0\theta} \right] \rho(0) = 0,$$

which yields $\rho(0) = (1, \rho_1, \rho_2)^T$, where

$$\begin{aligned} \rho_1 &= \frac{(i\omega_0 K + r_1 d^*)\beta_{23}m^* + \beta_{21}\alpha_{13}Kd^*m^*}{(i\omega_0 K + r_2 m^*)\alpha_{13}d^* - \alpha_{12}\beta_{23}Kd^*m^*}, \\ \rho_2 &= \frac{-\alpha_{12}\beta_{21}K^2d^*m^* - (i\omega_0 K + r_1 d^*)(r_2 m^* + i\omega_0 K)}{(i\omega_0 K + r_2 m^*)\alpha_{13}Kd^* - \alpha_{12}\beta_{23}K^2d^*m^*}. \end{aligned}$$

Similarly, it can be verified that $\rho^*(s) = D(1, \rho_1^*, \rho_2^*)e^{i\omega_0 s}$ is the eigenvector of M^* corresponding to $-i\omega_0$, with

$$\begin{aligned} \rho_1^* &= \frac{(-i\omega_0 K + r_1 d^*)\beta_{23}m^* + \beta_{21}\alpha_{13}Kd^*m^*}{(-i\omega_0 K + r_2 m^*)\alpha_{13}d^* - \alpha_{12}\beta_{23}Kd^*m^*}, \\ \rho_2^* &= \frac{-\alpha_{12}\beta_{21}K^2d^*m^* + (i\omega_0 K - r_1 d^*)(r_2 m^* - i\omega_0 K)}{(-i\omega_0 K + r_2 m^*)\alpha_{13}Kd^* - \alpha_{12}\beta_{23}K^2d^*m^*}. \end{aligned}$$

Using previous results, we have

$$\begin{aligned} \langle \rho^*(s), \rho(0) \rangle &= \bar{D}(1, \bar{\rho}_1^*, \bar{\rho}_2^*)(1, \rho_1, \rho_2)^T - \int_{-\tau_1^*}^0 \int_{\xi=0}^{\theta} (1, \bar{\rho}_1^*, \bar{\rho}_2^*)e^{-i\omega_0(\xi-\theta)} dg(\theta)(1, \rho_1, \rho_2)^T e^{i\omega_0\xi} d\xi \\ &= 1 + \rho_1 \bar{\rho}_1^* + \rho_2 \bar{\rho}_2^* - \int_{-\tau_1^*}^0 (1, \bar{\rho}_1^*, \bar{\rho}_2^*)\theta e^{i\omega_0\theta} dg(\theta)(1, \rho_1, \rho_2)^T \\ &= 1 + \rho_1 \bar{\rho}_1^* + \rho_2 \bar{\rho}_2^* - \int_{-\tau_1^*}^0 (1, \bar{\rho}_1^*, \bar{\rho}_2^*)\theta e^{i\omega_0\theta} dg(\theta)(1, \rho_1, \rho_2)^T \\ &= 1 + \rho_1 \bar{\rho}_1^* + \rho_2 \bar{\rho}_2^* + \tau_1^* \delta_1 \bar{\rho}_2^* c^* e^{-i\omega_0\tau_1^*} + \tau_2^0 \delta_1 \rho_1 \bar{\rho}_2^* c^* e^{-i\omega_0\tau_2^0}. \end{aligned}$$

By the fact that $\langle \rho^*, \rho \rangle = 1$, \bar{D} is written in the following form

$$\bar{D} = \frac{1}{1 + \rho_1 \bar{\rho}_1^* + \rho_2 \bar{\rho}_2^* + \tau_1^* \delta_1 \bar{\rho}_2^* c^* e^{-i\omega_0\tau_1^*} + \tau_2^0 \delta_1 \rho_1 \bar{\rho}_2^* c^* e^{-i\omega_0\tau_2^0}}.$$

To determine the direction of Hopf bifurcation and the stability of the periodical solutions, the Hassard algorithm is used [13] and the same calculation steps in [9], and we get the following coefficients

Table 6. Expressions for the parameters in (13).

Parameter	Expression
σ_{11}	$\frac{-r_1}{K} - \alpha_{12}\rho_1 - \alpha_{13}\rho_2$
σ_{21}	$\frac{-r_2}{K}\rho_1^2 + \beta_{21}\rho_1 - \beta_{23}\rho_1\rho_2$
σ_{31}	$-\frac{r_3}{K}\rho_2^2 + \lambda_{31}\rho_2 + \lambda_{32}\rho_1\rho_2 - \delta_1\rho_2e^{-i\omega_0\tau_1^*} - \delta_2\rho_1\rho_2e^{i\omega_0\tau_2^0}$
σ_{12}	$\frac{-2r_1}{K} - \alpha_{12}(\rho_1 + \bar{\rho}_1) - \alpha_{13}(\rho_2 + \bar{\rho}_2)$
σ_{22}	$-\frac{2r_2}{K}\rho_1\bar{\rho}_1 + \beta_{21}(\rho_1 + \bar{\rho}_1) - \beta_{23}(\rho_1\bar{\rho}_2 + \rho_2\bar{\rho}_1)$
σ_{32}	$-\frac{2r_3}{K}\rho_2\bar{\rho}_2 + \lambda_{31}(\rho_2 + \bar{\rho}_2) + \lambda_{32}(\rho_1\bar{\rho}_2 + \rho_2\bar{\rho}_1)$ $-\delta_1(\bar{\rho}_2e^{-i\omega_0\tau_1^*} + \rho_2e^{i\omega_0\tau_1^*}) - \delta_2(\rho_1\bar{\rho}_2e^{-i\omega_0\tau_2^0} + \bar{\rho}_1\rho_2e^{i\omega_0\tau_2^0})$
σ_{13}	$-\frac{r_1}{K} - \alpha_{12}\bar{\rho}_1 - \alpha_{13}\bar{\rho}_2$
σ_{23}	$\frac{-r_2}{K}\bar{\rho}_1^2 + \beta_{21}\bar{\rho}_1 - \beta_{23}\bar{\rho}_1\bar{\rho}_2$
σ_{33}	$-\frac{r_3}{K}\bar{\rho}_2^2 + \lambda_{31}\bar{\rho}_2 + \lambda_{32}\bar{\rho}_1\bar{\rho}_2 - \delta_1\bar{\rho}_2e^{i\omega_0\tau_1^*} - \delta_2\bar{\rho}_1\bar{\rho}_2e^{i\omega_0\tau_2^0}$
σ_{14}	$\frac{-r_1}{K}(2\omega_{11}^1(0) + \omega_{20}^2(0))$ $-\alpha_{12}\left(\omega_{11}^2(0) + \frac{\omega_{20}^2(0)}{2} + \bar{\rho}_1\frac{\omega_{20}^1(0)}{2} + \rho_1\omega_{11}^1(0)\right)$ $-\alpha_{13}\left(\omega_{11}^3(0) + \frac{\omega_{20}^3(0)}{2} + \bar{\rho}_2\frac{\omega_{20}^1(0)}{2} + \rho_2\omega_{11}^1(0)\right)$
σ_{24}	$-\frac{r_2}{K}(\bar{\rho}_1w_{20}^2(0) + 2\rho_1w_{11}^2(0))$ $+\beta_{21}\left(w_{11}^2(0) + \frac{w_{20}^2(0)}{2} + \bar{\rho}_1\frac{w_{20}^1(0)}{2} + \rho_1w_{11}^1(0)\right)$ $-\beta_{23}\left(\rho_1w_{11}^3(0) + \bar{\rho}_1\frac{w_{20}^3(0)}{2} + \bar{\rho}_2\frac{w_{20}^2(0)}{2} + \rho_2w_{11}^2(0)\right)$
σ_{34}	$\frac{-r_3}{K}(2\rho_2w_{11}^3(0) + \bar{\rho}_2w_{20}^3(0))$ $+\lambda_{31}\left(w_{11}^3(0) + \frac{w_{20}^3(0)}{2} + \bar{\rho}_2\frac{w_{20}^1(0)}{2} + \rho_2w_{11}^1(0)\right)$ $+\lambda_{32}\left(\rho_1w_{11}^3(0) + \bar{\rho}_1\frac{w_{20}^3(0)}{2} + \bar{\rho}_2\frac{w_{20}^2(0)}{2} + \rho_2w_{11}^2(0)\right)$ $-\delta_1\left(w_{11}^3(0)e^{-i\omega_0\tau_1} + \frac{w_{20}^3(0)}{2}e^{i\omega_0\tau_1} + \frac{w_{20}^1(-\tau_1^*)}{2}\bar{\rho}_2 + w_{11}^1(-\tau_1^*)\rho_2\right)$ $-\delta_2\left(\rho_1w_{11}^3(0)e^{-i\omega_0\tau_2^0} + \bar{\rho}_1\frac{w_{20}^3(0)}{2}e^{i\omega_0\tau_2^0} + \bar{\rho}_2\frac{w_{20}^2(-\tau_2^0)}{2} + \rho_2w_{11}^2(-\tau_1^*)\right)$

Therefore, we use this table to calculate the coefficients g_{ij} ,

$$\begin{aligned}
 g_{20} &= 2\bar{D}(\sigma_{11} + \bar{\rho}_1^*\sigma_{21} + \bar{\rho}_2^*\sigma_{31}), \\
 g_{11} &= \bar{D}(\sigma_{12} + \bar{\rho}_1^*\sigma_{22} + \bar{\rho}_2^*\sigma_{32}), \\
 g_{02} &= 2\bar{D}(\sigma_{13} + \bar{\rho}_1^*\sigma_{23} + \bar{\rho}_2^*\sigma_{33}), \\
 g_{21} &= 2\bar{D}(\sigma_{14} + \bar{\rho}_1^*\sigma_{24} + \bar{\rho}_2^*\sigma_{34}).
 \end{aligned} \tag{13}$$

However

$$\begin{aligned}
 W_{20}(\theta) &= \frac{ig_{20}}{\omega_0}\rho(\theta)e^{i\omega_0\theta} + \frac{i\bar{g}_{20}}{3\omega_0}\bar{\rho}(\theta)e^{-i\omega_0\theta} + \Lambda_1e^{2i\omega_0\theta}, \\
 W_{11}(\theta) &= -\frac{ig_{11}}{\omega_0}\bar{\rho}(\theta)e^{i\omega_0\theta} + \frac{i\bar{g}_{11}}{\omega_0}\bar{\rho}(\theta)e^{-i\omega_0\theta} + \Lambda_2,
 \end{aligned}$$

where Λ_1 and Λ_2 are constant vectors and they are determined by the following equations

$$\Lambda_1 = 2 \begin{pmatrix} 2i\omega_0 + \frac{r_1 d^*}{K} & \alpha_{12} d^* & \alpha_{13} d^* \\ -\beta_{21} m^* & 2i\omega_0 + \frac{r_2 m^*}{K} & \beta_{23} m^* \\ -\lambda_{31} c^* + \delta_1 c^* e^{-2i\omega_0 \tau_1^*} & -\lambda_{32} c^* + \delta_2 c^* e^{-2i\omega_0 \tau_2^0} & 2i\omega_0 + \frac{r_3 c^*}{K} \end{pmatrix}^{-1} \begin{pmatrix} \sigma_{11} \\ \sigma_{21} \\ \sigma_{31} \end{pmatrix},$$

$$\Lambda_2 = \begin{pmatrix} \frac{r_1 d^*}{K} & \alpha_{12} d^* & \alpha_{13} d^* \\ -\beta_{21} m^* & \frac{r_2 m^*}{K} & \beta_{23} m^* \\ (\delta_1 - \lambda_{31}) c^* & (\delta_2 - \lambda_{32}) c^* & \frac{r_3 c^*}{K} \end{pmatrix}^{-1} \begin{pmatrix} \sigma_{12} \\ \sigma_{22} \\ \sigma_{32} \end{pmatrix}.$$

One can see that each g_{ij} can be expressed by the parameters. Thus we can compute the following results

$$\begin{aligned} C_1(0) &= \frac{i}{2\omega_0} \left(g_{11}g_{20} - 2|g_{11}|^2 - \frac{|g_{02}|^2}{3} \right) + \frac{g_{21}}{2}, \\ \eta_2 &= -\frac{\operatorname{Re}(C_1(0))}{\operatorname{Re}(\lambda'(\tau_2^0))}, \quad \beta_2 = 2\operatorname{Re}(C_1(0)), \\ T_2 &= -\frac{\operatorname{Im}(C_1(0)) + \mu_2 \operatorname{Im}(\lambda'(\tau_2^0))}{\omega_0}. \end{aligned} \quad (14)$$

6. Discussion

This section presents the results of the carried out simulations, and deals with a concrete example to illustrate the theoretical results obtained in the previous sections.

The figures included below show the variation of *Dinoflagellates*, *Mussels* and *Crabs* over time in order to analyse the stability of these species in the presence of the fishing and toxicity effect. The values of the parameters used in the relevant bioeconomic model are affected as follows, the values of these parameters are based on INRH report.

The system studied admits a point of interior equilibrium $P^* = (9.6202, 11.2368, 9.6561)$, here we vary the delays and we observe the stability of the system. To do this, we have discussed the predefined four cases in ten scenarios.

The first case, presented in Figs.1a and 1b, indicates that the affectation by toxicity is instantaneous, namely $\tau_1 = \tau_2 = 0$. Indeed, the simulations performed demonstrate the verification of the stability condition concerning the system through the selected parameters. In fact, we have $h_2 = 6.0313 > 0$, $h_1 = 68.6426 > 0$, $h_0 = 148.0407 > 0$ and $h_1 h_2 - h_0 = 265.9602 > 0$, then the conditions of Routh–Hurwitz hold. We have showed that the point P^* is locally asymptotic stable in Fig. 1a by using as initial value the point (9, 11, 9). In these graphs, we have unsaturated any initial points. Subsequently we noticed that the curve converges towards the equilibrium point of the P^* system, a point which is represented as a global attractor in Fig. 1b.

In the second case, we consider the system with one delay, and we discuss the stability of the equilibrium point in four scenarios. In the first one, we have $r_1 = 43156 > 0$ and $\Delta = -7.103 < 0$, then the conditions (i) mentioned in Theorem 6 are satisfied, which gives the stability of P^* for all $\tau_1 \geq 0$ and $\tau_2 = 0$ with $K = 30$. Also, we obtain the same result if $\tau_1 = 0$ and $\tau_2 \geq 0$. However, when the value of carrying capacity is changed, then the system loses its stability since the theorem condition (i) are not satisfied in this scenario. To prove that graphically, we choose $K = 100$ with $\tau_1 = 0.05$, $\tau_2 = 0$ and $\tau_1 = 0.5$, $\tau_2 = 0$.

Table 7. Bioeconomic parameters and their values.

Parameter	Value	Parameter	Value
r_1	0.73	α_{12}	0.03
r_2	0.65	α_{13}	0.5
r_3	0.39	β_{21}	0.01
E_1	10	β_{23}	0.45
E_2	10	λ_{31}	0.15
E_3	100	λ_{32}	0.18
q_1	0.0002	δ_1	0.0023
q_2	0.0001	δ_2	0.0016
q_3	0.015	K	30

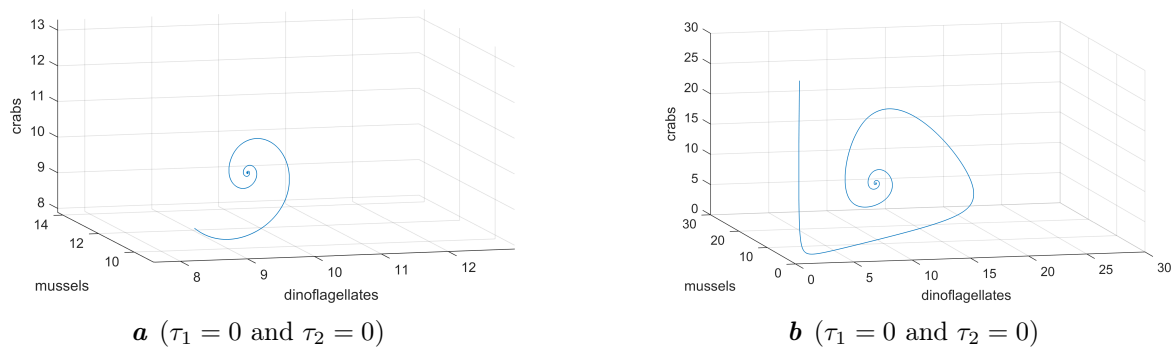


Fig. 1. Phase portrait of system solution without delay.

From the outset, the second case consists of two Figs. 2a and 2b in which the condition (i) in Theorem 6 is verified, for Fig. 2a it is assumed that $\tau_1 = 0.5 > 0$ and $\tau_2 = 0$, while in Fig. 2b $\tau_1 = 0$ and $\tau_2 = 0.5 > 0$ are set. After the simulations, it is attested that for any initial point, the system tends towards the equilibrium point P^* . Thus, the system maintains its stability.

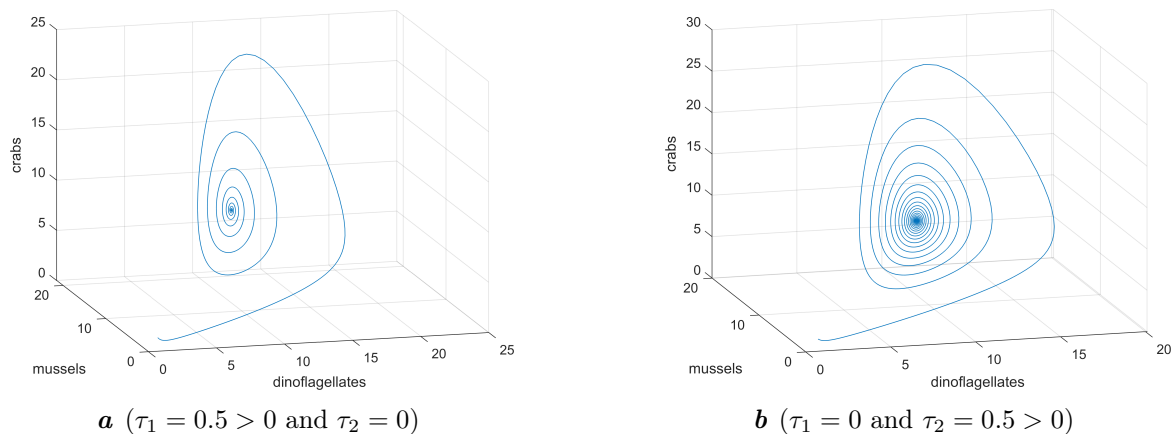


Fig. 2. Phase portrait of system solution when $\tau_1 > 0$ and $\tau_2 = 0$ or $\tau_1 = 0$ and $\tau_2 > 0$.

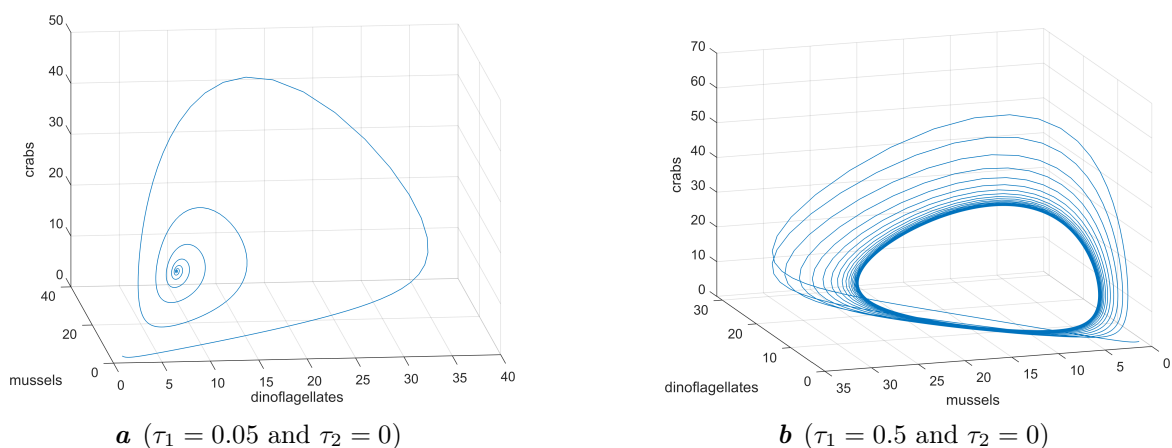


Fig. 3. Phase portrait of system solution when $\tau_1 > 0$, $\tau_2 = 0$ and $K = 100$.

In fact, when the K value is changed from 30 to 100, the condition (i) in Theorem 6 is no longer checked except for the others. However, the condition (ii) holds. Indeed, $s_1 = 4341 > 0$, $\Delta = 8150.4 > 0$, $v_1 = 88.31 > 0$ and $g(v_1) = -1111.5 < 0$. Then, Eq. (8) has two positive roots which give us the following critical values $\tau_{11}^{(j)} = 0.409 + 0.647j$ and $\tau_{12}^{(j)} = 0.684 + 0.751j$ for $(j = 0, 1, \dots)$.

With $\alpha'(\tau_{11}^{(j)}) > 0$ and $\alpha'(\tau_{12}^{(j)}) < 0$. So, we have the following stability interval $\tau_1 \in [0, 0.409) \cup (0.684, 1.056) \cup (1.435, 1.757) \cup (2.186, 2.35) \cup (2.937, 2.997)$. However, when we choose $\tau_1 = 0.05$ belonging to the stability interval, we observe that the system converges towards a new equilibrium point $P^* = (7.8209, 12.2596, 13.1213)$. However, for $\tau_1 = 0.5$ not belonging to the stability interval, we note the loss of stability and the appearance of periodic solutions.

In the third case, we assume that $\tau_1 = \tau_2 = \tau$, and we notice the stability of P^* when τ is in the interval of stability; in other words, if the condition of Theorem 6 does not hold, the system undergoes a Hopf bifurcation.

For the third case, two Figs. 4a and 4b illustrate the results of the simulations and we first consider that $\tau_1 = \tau_2 = \tau$. For graph (f) we set $\tau = 0.3$ and we end up concluding the stability of the system, while in graph (g) we choose $\tau = 0.5$, in other words, τ exceeds the critical time of the bifurcation of Hopf, then the system loses its stability. Therefore, the appearance of periodic solutions around the equilibrium point P^* is asserted.

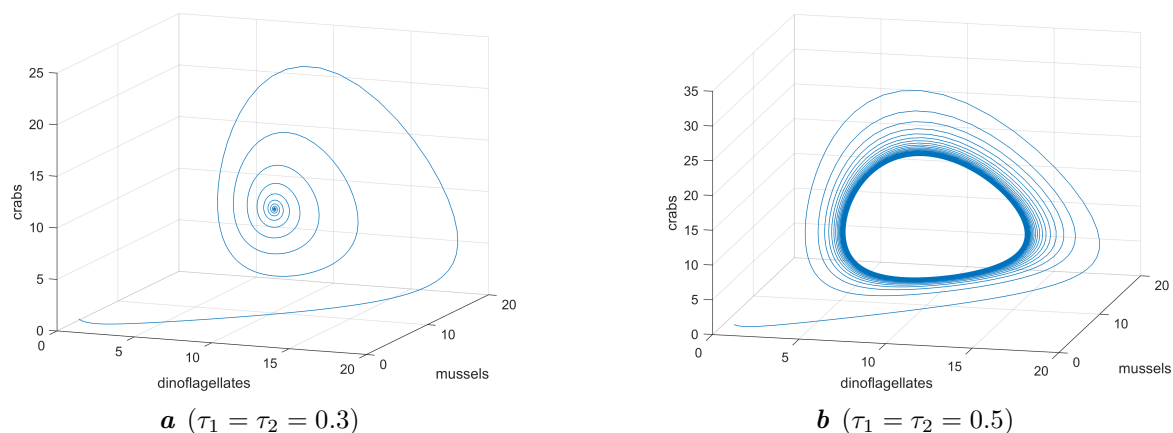


Fig. 4. Phase portrait of system solution when $\tau_1 = \tau_2 = 0.3$ and $\tau_1 = \tau_2 = 0.5$.

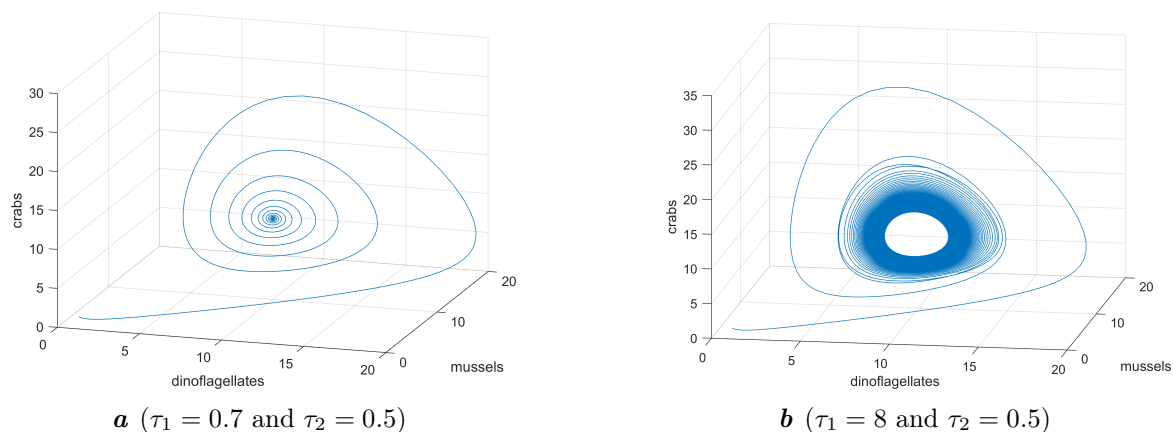


Fig. 5. Phase portrait of system solution when $\tau_1 = 0.7$ and $\tau_2 = 0.5$ or $\tau_1 = 8$ and $\tau_2 = 0.5$.

In the last case, we consider the system with two different delays. As a main result, we found the appearance of periodic solutions when τ_1 or τ_2 are outside the stability interval, in other words if the conditions mentioned in Theorem 7 are not satisfied.

Admittedly, in the fourth case we have $\tau_1 > 0$ and $\tau_2 > 0$ such as $\tau_1 \neq \tau_2$ and two Figs. 5a and 5b. Figure 5a starts from $\tau_2 = 0.5$ and $\tau_1 = 0.7$, i.e., they belong to the stability interval. After the simulations, it is claimed that the curve showing the evolution of the biomass of the species converges towards the equilibrium point. In other words, the result is the stability of the system. However, Fig. 5b poses $\tau_1 = 8$ and $\tau_2 = 0.5$ that are outside the stability interval. As a result, for $\tau_2 = 0.5$, we

have $\tau_1^0 = 1.0573$, $\beta_2 < 0$ and $\eta_2 > 0$. Then, when $\tau_1 > \tau_1^0$ it is observed that the system loses its stability and stable periodic solutions appear.

7. Conclusion

In this study, the focus is on modeling the interaction between dinoflagellates, mussels, and crabs through a delayed dynamic system. Thus, an analysis of the system is performed to identify its bifurcations. In the end, we find that the stability of the system is directly related to the delay designating the allocation time by the toxins and its belonging to the stability interval. When it is lost, periodic solutions appear. Research avenues appeared to consider a rate of delay not constant and dependent on the biomass of species or to study bifurcations related to other parameters for the preservation of species and all marine biodiversity.

-
- [1] El Foutayeni Y., Bentounsi M., Agmour I., Achtaich N. Bioeconomic model of zooplankton–phytoplankton in the central area of Morocco. *Modeling Earth Systems and Environment*. **6**, 461–469 (2020).
 - [2] El Foutayeni, Y., M. Khaladi, and A. Zegzouti. Profit maximization of fishermen exploiting two fish species in competition. *Amer. J. Comput. Appl. Math.* to appear (2023).
 - [3] El Foutayeni Y., Khaladi M. A generalized bio-economic model for competing multiple-fish populations where prices depend on harvest. *Journal of Advanced Modeling and Optimization*. **14** (3), 531–542 (2012).
 - [4] El Foutayeni Y., Khaladi M. A bio-economic model of fishery where prices depend harvest. *Journal of Advanced Modeling and Optimization*. **14** (3), 543–555 (2012).
 - [5] Bentounsi M., Agmour I., Achtaich N., El Foutayeni Y. The impact of price on the profits of fishermen exploiting tritrophic prey–predator fish populations. *International Journal of Differential Equations*. **13**, 2381483 (2018).
 - [6] Bentounsi M., Agmour I., Achtaich N., El Foutayeni Y. Intrinsic growth rates influence on the net economic rents of fishermen. *International Journal of Dynamical Systems and Differential Equations*. **9** (4), 362–379 (2019).
 - [7] Agmour I., Achtaich N., El Foutayeni Y. Carrying capacity influence on the incomes of seiners exploiting marine species in the Atlantic coast of Morocco. *Mathematical Biosciences*. **305**, 10–17 (2018).
 - [8] Agmour I., Achtaich N., El Foutayeni Y. Stability analysis of a competing fish populations model with the presence of a predator. *International Journal of Nonlinear Science*. **26** (2), 108–121 (2018).
 - [9] Bentounsi M., Agmour I., Achtaich N., El Foutayeni Y. The Hopf bifurcation and stability of delayed predator–prey system. *Computational and Applied Mathematics*. **37** (5), 5702–5714 (2018).
 - [10] Song Y., Wei J. Bifurcation analysis for Chen’s System with delayed feedback and its application to Control of chaos. *Chaos, Solitons & Fractals*. **22** (1), 75–91 (2004).
 - [11] Ruan S., Wei J. On the zeros of transcendental functions with applications to stability of delay differential equations with two delays. *Dynamics of Continuous, Discrete & Impulsive Systems A*. **10** (6), 863–874 (2003).
 - [12] Hale J. K. *Theory of Functional Differential Equations*. Springer, New York (1977).
 - [13] Hassard B. D., Kazarinoff N. D., Wan Y.-H. *Theory and applications of hopf bifurcation*. Cambridge University Press, Cambridge (1981).

Дослідження біфуркації Хопфа для уповільненої тритрофної системи: динофлагеляти, мідії та краби

Хафдане М.¹, Агмур І.¹, Ель Футаєні Ю.^{1,2}

¹Лабораторія аналізу, моделювання та симулювання, Університет Хасана II, Марокко

²Відділ математичного та комп'ютерного моделювання складних систем, IRD, Франція

У статті розглянуто дискретну динамічну систему зі затримкою з трьома морськими видами: жертва, хижак та суперхижак. Враховано не лише ефект токсичності здобичі, але і негативний ефект надмірного ловіння перелічених видів. Дослідження моделі полягає в пошуку рівноваги за допомогою аналізу власних значень, існування біфуркацій Хопфа у внутрішніх рівновагах, визначення напрямку та аналізу стійкості біфуркації Хопфа з використанням теорії нормальної форми та центрального многовиду. Наведено декілька прикладів із чисельним моделюванням, які ілюструють результати для різних значень затримки.

Ключові слова: *хижак-здобич; аналіз стійкості; біфуркація Хопфа; дискретна затримка; рибальське зусилля.*